Stem Cell Reports
Article

OPEN ACCESS

Heterogeneity of SOX9 and HNF1β in Pancreatic Ducts Is Dynamic

Habib Rezanejad,[1,3] Limor Ouziel-Yahalom,[1,3] Charlotte A. Keyzer,[1] Brooke A. Sullivan,[1] Jennifer Hollister-Lock,[1] Wan-Chun Li,[1] Lili Guo,[1] Shaopeng Deng,[2] Ji Lei,[2] James Markmann,[2] and Susan Bonner-Weir[1,*]

[1]Section of Islet Cell and Regenerative Biology, Joslin Diabetes Center, Harvard Medical School, Boston, MA 02215, USA
[2]Massachusetts General Hospital, Department of Surgery, Harvard Medical School, Boston 02114, USA
[3]Co-first author
*Correspondence: susan.bonner-weir@joslin.harvard.edu
https://doi.org/10.1016/j.stemcr.2018.01.028

SUMMARY

Pancreatic duct epithelial cells have been suggested as a source of progenitors for pancreatic growth and regeneration. However, genetic lineage-tracing experiments with pancreatic duct-specific Cre expression have given conflicting results. Using immunofluorescence and flow cytometry, we show heterogeneous expression of both HNF1β and SOX9 in adult human and murine ductal epithelium. Their expression was dynamic and diminished significantly after induced replication. Purified pancreatic duct cells formed organoid structures in 3D culture, and heterogeneity of expression of *Hnf1β* and *Sox9* was maintained even after passaging. Using antibodies against a second cell surface molecule CD51 (human) or CD24 (mouse), we could isolate living subpopulations of duct cells enriched for high or low expression of *HNF1β* and *SOX9*. Only the CD24^{high} (*Hnfβ* ^{high}/*Sox9* ^{high}) subpopulation was able to form organoids.

INTRODUCTION

Two distinct strategies of pancreatic β cell replacement offer promise to counter the loss of insulin-producing β cells in diabetes: (1) from an exogenous source of glucose-responsive, insulin-secreting cells from stem/progenitor cells; and (2) endogenously by activating regeneration. The β cells could be replenished through the self-replication of existing β cells (Dor et al., 2004) and/or differentiation from other pancreatic cell types (Baeyens et al., 2014; Bonner-Weir et al., 2004; Pan et al., 2013). Self-renewal of β cells is an important mechanism of β cell mass expansion postnatally (Dor et al., 2004; Teta et al., 2007), but is less active in adults (Thorel et al., 2010). There is considerable evidence for differentiation from non-islet cell progenitors (neogenesis) (reviewed in Bonner-Weir et al., 2010), as well as transdifferentiation from other islet cell types (Al-Hasani et al., 2013; Chera et al., 2014; Collombat et al., 2009; Courtney et al., 2013; Thorel et al., 2010), whereas the existence of a true pancreatic stem cell has little support (Seaberg et al., 2004).

If there were newly differentiated endocrine cells after birth, the favored "cell of origin" is within the pancreatic ducts, whether by a general plasticity across the ductal tree, within a category of duct, or a subpopulation of scattered cells. One possibility is the rare subpopulation of aldehyde dehydrogenase 1^{high} centroacinar cells that *in vitro* can self-renew and differentiate toward both endocrine and acinar cells (Rovira et al., 2010); however, their rarity and location preclude their being the only source. Embryonic pancreatic progenitors have been postulated to have a complex transcriptional network of *Sox9, Hnf1β/Tcf2, Foxa2/Hnf3β*, and *Hnf6/Onecut1* that is maintained by cross-regulation of these transcription factors (Lynn et al., 2007). HNF1β plays a key regulatory role in endoderm development and becomes restricted in expression in the duct epithelia of several organs, including the pancreas (Cereghini et al., 1992). Its expression is directly regulated by SOX9 (Lynn et al., 2007; Seymour et al., 2007, 2008). SOX9 has been shown to be required for the maintenance of multipotent pancreatic progenitor cell pool in the early embryonic pancreas (Seymour et al., 2007) and to give rise to both exocrine and endocrine cells in a dose-dependent manner.

Lineage-tracing studies using inducible *Hnf1β* and *Sox9* promoters to mark duct progeny concluded that pancreatic duct cells give rise to β cells only during embryogenesis and not after birth or partial duct ligation (PDL) (Furuyama et al., 2011; Kopp et al., 2011; Solar et al., 2009). However, subsequent studies using the same *Sox9Cre^{ERT}* mice found that ductal cells could give rise to new β cells in adults under certain conditions (Zhang et al., 2016). The latter findings are in agreement with our study using the *Carbonic anhydrase II* (CAII) promoter that demonstrated a ductal origin of all pancreatic cell types in normal neonatal growth and of islets after PDL (Inada et al., 2008). Other evidence of a ductal origin of new β cells postnatally used molecular tracing of the pre-endocrine marker NGN3 and showed activation of NGN3^{+} cells within the pancreatic duct epithelium after PDL (Xu et al., 2008). Moreover, when isolated and transplanted into fetal pancreatic explants, these NGN3^{+} cells had the ability to differentiate into insulin-expressing cells. More recently (Pan et al., 2013), inducible lineage tracing of *Ptf1a*-derived cells

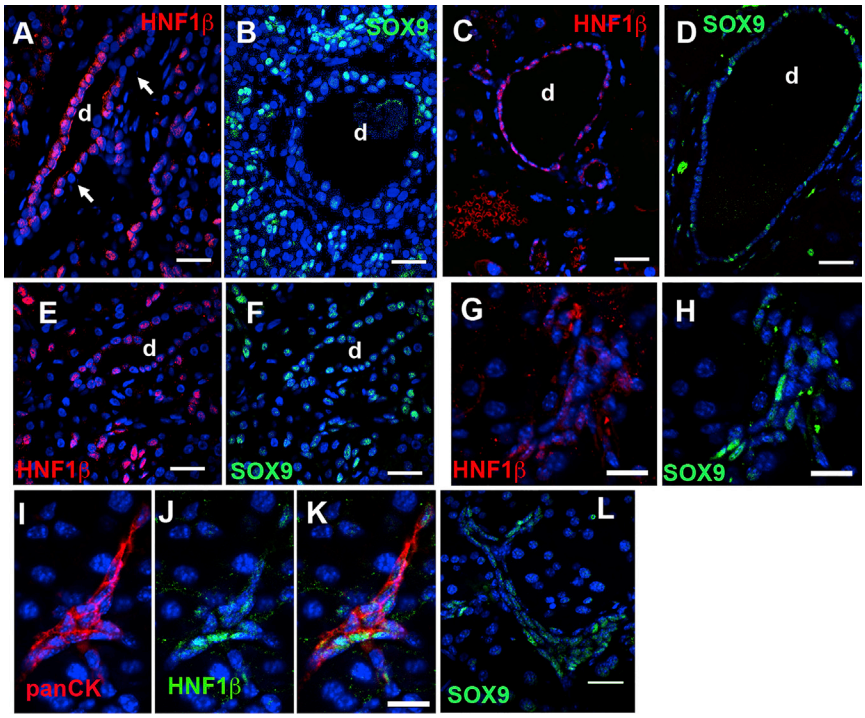

Figure 1. Heterogeneity of HNF1β and SOX9 Proteins in Adult Human and Mouse Pancreas

In humans, HNF1β (red) (A) has heterogeneous expression even within the same duct and some cells have undetectable levels (white arrows); SOX9 (green) expression (B) is also heterogeneous, stronger in small terminal ducts than in larger ducts (center). Similarly, in mouse, higher and more homogeneous staining of HNF1β (C) and lower, more heterogeneous SOX9 staining (D), is seen in large ducts than in small ducts. Heterogeneity of HNF1β and SOX9 expression only partially overlaps in human (E and F) and mouse (G and H) pancreas. Double-stained SOX9 (green) HNF1β (red) sections shown as split channels. In mouse small terminal ducts (Pan Cytokeratin red), some cells present high levels of HNF1β (green), and the rest are either HNF1β^{low} or HNF1β^{undetectable} (I–K), whereas SOX9 (L) is expressed in most. DAPI (blue)-stained nuclei. d, ducts. Scale bars, 25 μm (A–F and L), 50 μm (G, H, and K).

showed an acinar-to-duct transition rapidly after PDL followed more slowly (weeks) with some labeled β cells; this process was faster and more robust if there was hyperglycemia. Another study showed the severity and type of pancreatic injury determined which cells regenerated (Criscimanna et al., 2011), with both islet and acinar cells regenerated from pancreatic duct cells when both the acinar and β cells were ablated (*Pdx^{cre}ROSA^{DTR}* transgenic mice treated with diphtheria toxin). Further evidence that ducts can serve as β cell progenitors in the adult mouse comes from a series of papers from Collombat (Al-Hasani et al., 2013; Collombat et al., 2009; Courtney et al., 2013) using genetic manipulations in glucagon-expressing α cells (overexpression of PAX4, deletion of ARX) that resulted in their becoming β cells. With the loss of α cells, duct epithelial cells continuously formed new α cells that then converted to β cells.

Yet a controversy of a ductal origin of new β cells has arisen from the unexplained discrepancies found with lineage-tracing experiments. As an alternative to a technical issue of the Cre-lox system, such as a very low recombination in the neonatal period (embryonic day [E] 18.5 to postnatal day [P] 5) in the inducible *Hnf1β* and *Sox9* mice (being only 10%–20%) (Kushner et al., 2010), or the use of regulatory sequences important for maintaining an undifferentiated state as the promoter (Beer et al., 2016), we hypothesized that a heterogeneity of HNF1β and SOX9 expression within the adult pancreatic ductal epithelium results in cells of varying plasticity, such that only a subpopulation has the potential for multipotency.

Here we show heterogeneous expression of both HNF1β and SOX9 in adult human and murine ductal epithelium with dynamic expression. We could isolate living subpopulations of duct cells enriched for high or low expression of *Hnf1β* and *Sox9* using fluorescence-activated cell sorting (FACS). These subpopulations differ in their gene expression, ability to expand and to form 3D organoids in culture, and to differentiate toward a progenitor phenotype.

RESULTS

Heterogeneous Pattern of HNF1β and SOX9 Expression across the Human and Mouse Pancreatic Ductal Tree

Titration of the primary antibodies in immunofluorescent staining allowed us to detect variation in expression of HNF1β and SOX9 proteins in human (Figures 1A, 1B, 1E, and 1F) and mouse adult pancreatic ducts (Figures 1C, 1D, and 1G–1K). HNF1β staining was more intense and more homogeneous in larger ducts (Figures 1A and 1C) than in smaller ducts (Figures 1E and 1G), whereas SOX9 had greater homogeneity and intensity in small ducts (Figures 1F, 1H, and 1L) than in the larger ducts (Figures 1B and 1D). Analysis of their co-localization showed only partial overlap of SOX9 and HNF1β expression (Figures 1E–1H). Expression of both extended to the terminal ducts (Figures 1B and 1I–1L).

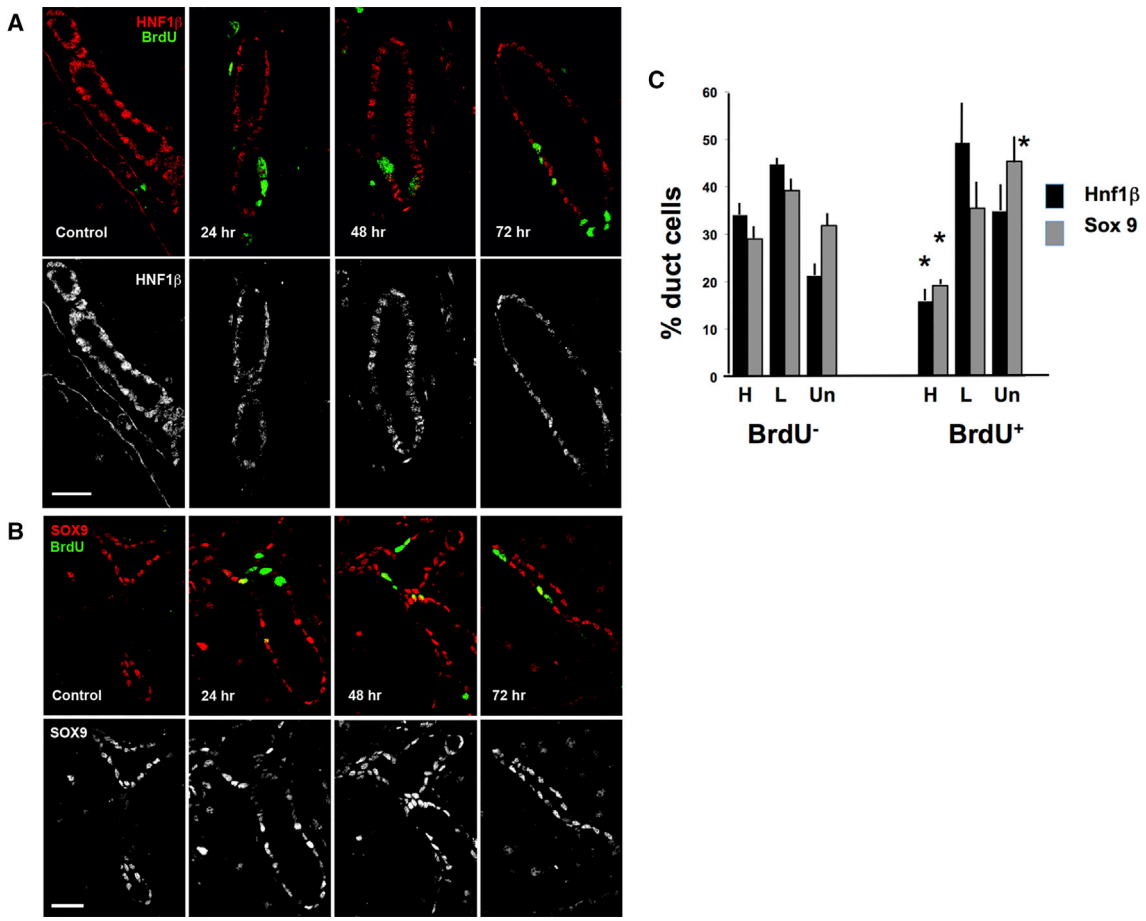

Figure 2. Replicating Duct Cells Have Reduced High-Intensity Staining for HNF1β and SOX9

(A and B) Eighteen hours after KGF administration, BrdU was injected and the animals were killed at different times of "chase." BrdU labeling significantly increased (24 hr, 8.9% ± 0.5%; 48 hr, 13.1% ± 0.8%; 72 hr, 14.6% ± 1.0%) in KGF-injected mice compared with controls (0.7% ± 0.4%; $p < 0.001$). BrdU, green (A and B); HNF1β, red (A); and SOX9, red (B) immunostaining shown merged (top) and as single channel (lower).

(C) Quantification showed that, in the replicating ($BrdU^+$) duct cells, the percentage of both $HNF1\beta^{high}$ and $SOX9^{high}$ cells decreased and $SOX9^{undetectable}$ significantly increased compared with quiescent ($BrdU^-$) at all time points. These proportions did not differ in Control and $BrDU^-$ cells at any time point so the values were combined; similarly the $BrdU^+$ did not differ at any time point and so were combined. n = 3 mice/group; 536–1,474 duct cells each time.

Data are means ± SEM. *$p < 0.05$. Scale bars, 25 μm.

HNF1β and SOX9 Expression after Replication

To determine whether HNF1β and SOX9 expression was dynamic and changed with replication, adult mice were injected with keratinocyte growth factor (KGF) to induce synchronous replication, and 18 hr later injected with bromodeoxyuridine (BrdU) to mark those cells that were replicating in response. At 24, 48, and 72 hr after the KGF injection, mice were killed and the pancreas analyzed for expression of HNF1β (Figure 2A) and SOX9 (Figure 2B) in divided ($BrdU^+$) and non-divided ($BrdU^-$) duct cells. BrdU labeling differed significantly across the time course (24 hr, 8.9% ± 0.5%; 48 hr, 13.1% ± 0.8%; 72 hr, 14.6% ± 1.0%) compared with the saline-treated controls (control, 0.7% ± 0.4%; $p < 0.001$). The increased BrdU labeling at 48 and 72 hr should reflect the daughter cells of those that initially became labeled between 18 and 24 hr after KGF injection. The percentage of duct cells expressing high, low, and undetectable HNF1β and SOX9 were quantified (Figure 2C). In quiescent ($BrdU^-$) cells at any time point analyzed, the proportion of these subpopulations did not differ compared with controls, so the time points were combined for further analysis. Similarly, among the replicated ($BrdU^+$) cells, the proportion of each subpopulation did not differ between the 24, 48, and 72 hr time points; they were combined. However, in replicating ($BrdU^+$) duct cells the percentage of $HNF1\beta^{high}$ and

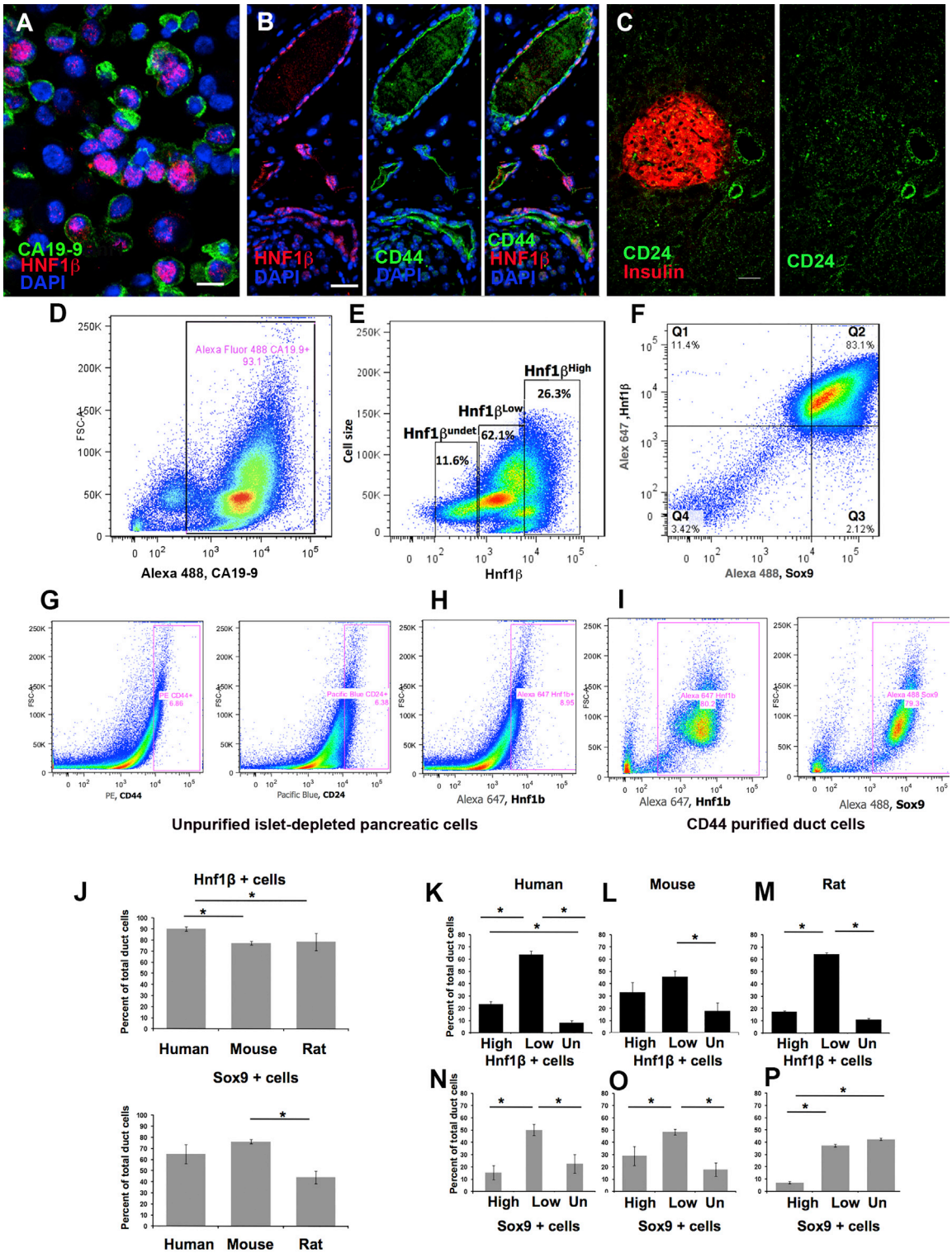

Figure 3. Flow Cytometry Analysis Showed Heterogeneous Pattern of HNF1β and SOX9

(A) Purified human duct cells stained for HNF1β (red) and CA19-9 (green). Scale bar, 10 μm.

(B) CD44 (green) is evident in mouse duct cells as identified by HNF1β (red). Scale bar, 20 μm.

(C) CD24 (green) is expressed in duct cells and not in adult islets (insulin, red). Scale bar, 25 μm.

(legend continued on next page)

SOX9^{high} cells was decreased and SOX9^{undetectable} significantly increased compared with the quiescent (BrdU^{-}). These data alone cannot distinguish between dynamic expression of these transcription factors and differential capacity for replication based on the expression levels.

Heterogeneous Pattern of HNF1β and SOX9 in Isolated Duct Cells

We have previously reported purification of adult human duct cells using the cell surface CA19-9 antibody and immunomagnetic sorting (Yatoh et al., 2007) (Figure 3A). Flow cytometric (FACS) separation confirmed the purity of the immunomagnetic duct isolation: 93.1% of the purified cells were CA19-9^{+} (Figure 3D). Using intracellular staining for HNF1β (Figure 3E) or SOX9 (data not shown) on fixed purified duct cells, it was possible to sort them according to their expression level. Nearly all purified human duct cells expressed HNF1β: 90.2% ± 2% (n = 8); and most expressed SOX9: 64.9% ± 8.5% (Figure 3F); the majority of CA19-9^{+} cells expressed HNF1β^{low} (66.6% ± 8.3%); the HNF1β^{high} fraction only 23.3% ± 5.6% and the HNF1β^{undetectable} fraction only 8.3% ± 5.0% (n = 8 donors). More human duct cells expressed SOX9^{low} (50.2% ± 4.6%) than SOX9^{high} (15.4% ± 5.8%). FACS of purified duct cells immunostained for both HNF1β and SOX9 (Figure 3F) confirmed the partial overlap seen on immunostained pancreatic sections: 60.7% ± 18.8% expressed both HNF1β and SOX9, 27.4% ± 18.8% expressed HNF1β, but not SOX9, and 10.9% ± 8.7% expressed neither (n = 5 donors).

A similar purification for rodent duct cells was obtained based on CD44 expression. Cell surface proteins that were selectively expressed at high mRNA levels in adult rat or human pancreatic ductal epithelium (S.B-W., unpublished data) were tested for selective protein expression in the ductal tree (and not in islets) by immunostaining and then by FACS sorting. In adult mouse pancreas, CD44 (Figure 3B) and CD24 (Figure 3C), a target of HNF1β (Senkel et al., 2005), are expressed selectively in duct cells (Wang et al., 2008). Again using intracellular staining for the transcription factors, FACS sorting of dispersed islet-depleted pancreatic cells on the basis of these cell surface markers gave 6.9% CD44^{+} (Figure 3G), 6.4% CD24^{+} cells (Figure 3G), 8.9% HNF1β^{+} (Figure 3H), and 12.2% SOX9^{+}. After immunomagnetic purification with antibody against CD44, 77.2% ± 1.7% were HNF1β^{+} (n = 6) (Figure 3I) and 79.3% SOX9^{+} (Figure 3I). Enrichment of rat duct cells was comparable (data not shown).

We found different frequency of expression of HNF1β and SOX9 in the isolated duct cells of the three species (Figure 3J). In both mouse and rat, significantly fewer duct cells expressed HNF1β than in human, whereas significantly more duct cells expressed SOX9 in mouse (76.3% ± 1.8%; n = 6) than rat (44% ± 5.6%; n = 3). In mouse there was no significance difference in the percentage of cells expressing HNF1β^{high} and HNF1β^{low}, whereas in both rat and human the HNF1β^{high} accounted for only about 20% of the total duct cells and HNF1β^{low} 60% (Figures 3K–3M). The percentage of cells expressing SOX9^{high}, SOX9^{low}, or SOX9^{undetectable} (Figures 3N–3P) differed among the three species. The implications of such differences may be the species difference in whether the replicative or neogeneic pathway of generating new β cells is dominant. In compensatory growth of β cells, replication has been shown to be dominant in adult mice (Teta et al., 2005, 2007), while neogenesis in adult humans appears to make an important contribution (Butler et al., 2010; Mezza et al., 2014; Yoneda et al., 2013).

Pancreatic Duct Cells Expand in 3D Culture and Form Organoids Reproducibly

Using only CD24-immunomagnetic purification, duct cells robustly formed multicellular epithelial organoids (Figure 4A) over a 2-week culture in growth factor-reduced (GFR) Matrigel and organogenesis medium (modified from Lee et al., 2013; Table S1); organoids were seen after a 3-day culture; by 13 days, about 15% of the embedded cells had formed organoids (n = 3). Of the formed

(D) Representative FACS confirms the purity with 93.1% isolated human CA19-9^{+} cells.
(E) Human CA19-9^{+} duct cells were fixed and stained with anti-HNF1β antibodies (x axis) plotted against forward scatter (cell size, y axis). HNF1β^{+} cells were gated using unstained and primary antibody controls and the percentage of HNF1β^{undetectable}, HNF1β^{low}, and HNF1β^{high} determined Fixed purified huamn ducts immunostained for Sox9 (x axis) and Hnf1β (y axis) (F).
(G–I) FACS of dispersed islet-depleted mouse pancreas, without purification, resulted in 6%–8% CD44^{+}, CD24^{+} cells (G), or HNF1β^{+} (H), whereas with CD44 purification and subsequent FACS for HNF1β or SOX9 immunostaining (I) duct cells were enriched to about 80%.
(J–P) Flow cytometry analysis comparison among human, mouse, and rat showing the mean percentage of duct cells isolated (J). Human (n = 8 donors; 266,473 cells/donor); mouse (initially purified by CD44 or CD24, n = 6, each pooled from 15 mice; 257,011 cells/experiment); rat pancreas (initially purified by CD44 or CD24, n = 4, each pooled from 15 rats; 70,799 cells/experiment). The percentages of HNF1β^{high}, HNF1β^{low}, HNF1β^{undetectable} in human (K), mouse (L), and rat (M), and of SOX9^{high}, SOX9^{low}, and SOX9^{undetectable} in human (N), mouse (O), and rat (P) varied among species. *p < 0.03.
Data are means ± SEM.

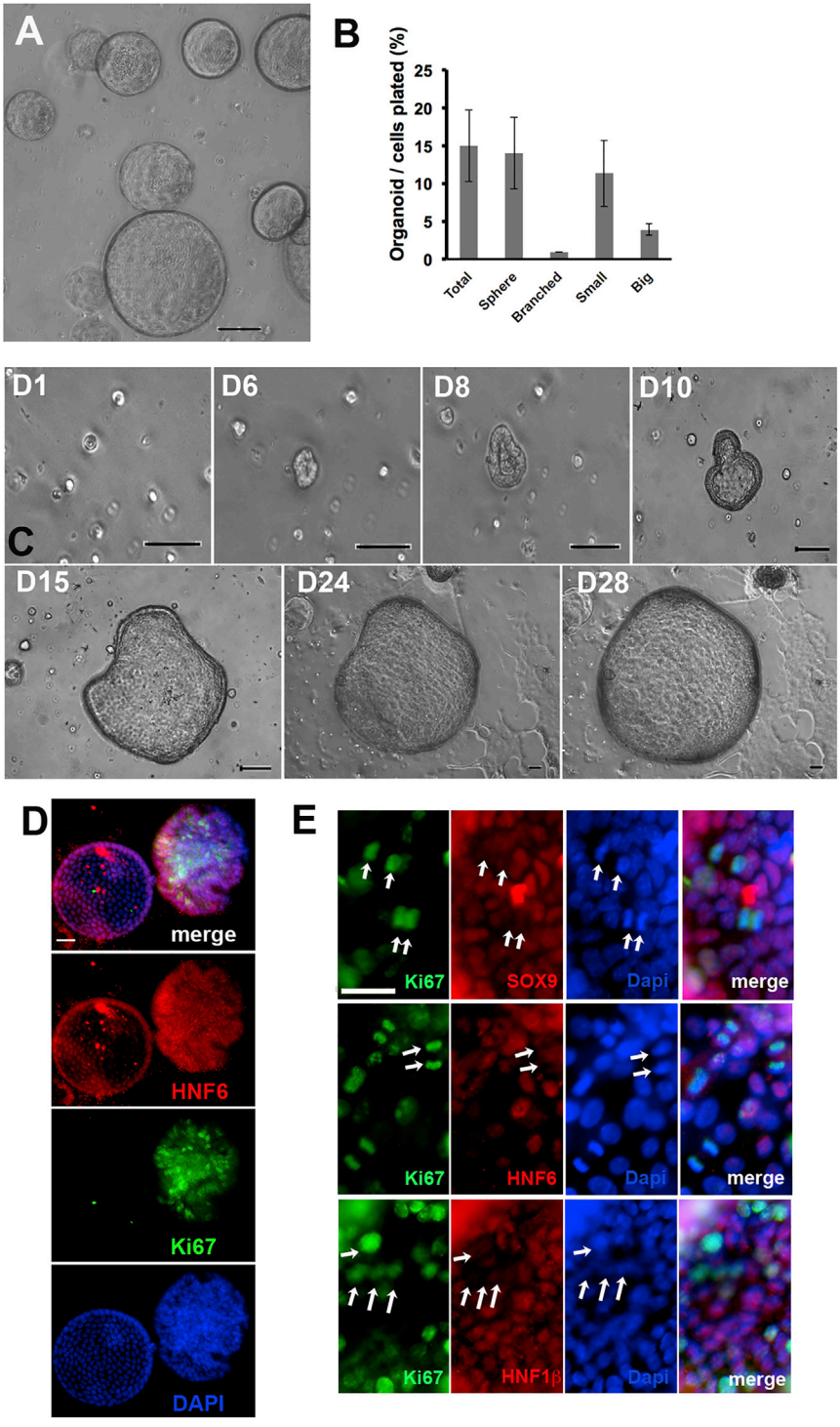

Figure 4. Murine Duct-Derived Organoids Show Heterogeneous Expression of HNF1β and SOX9 Proteins, with a Lower Expression in Proliferating Cells

(A) Duct cells robustly formed organoids after 2 weeks in Matrigel. n = 10 experiments. Scale bar, 200 μm.

(B) By 13 days of culture, about 15% of purified mouse duct cells formed organoids, mostly smooth spheres, but 7% of organoids were branched structures. n = 3 experiments, each at least 1,000 organoids counted.

(C) Representative time-lapse images over 28 days (D1–D28) of organoid formation from single mouse duct cells, confirming that the organoids arise from proliferation and not aggregation. n = 2 experiment, each with 5 fields followed. Scale bar, 100 μm.

(D) Proliferation marker Ki67 was highly, but variably, expressed in organoids: left, a smooth sphere; right, branched structure.

(E) Ki67$^+$ cells (arrows) had very low or undetectable expression of SOX9, HNF6, and HNF1β (n = 3 experiments).

Data are means ± SEM. Scale bars, 25 μm (D and E).

structures, most were hollow, well-rounded, smooth spheres, but about 7% were branched organoids, smaller and denser structures (Figure 4B). Organoids could be passaged at least 10 passages (n = 4). With passage, a higher frequency of organoids formed.

We analyzed organoid formation by time-lapse imaging over 4 weeks and confirmed that organoids formed from single cells (Figure 4C). Immunostaining of organoids at passage 2 and 3 confirmed that they were highly proliferative with 25% Ki67$^+$ cells, but this varied among organoids

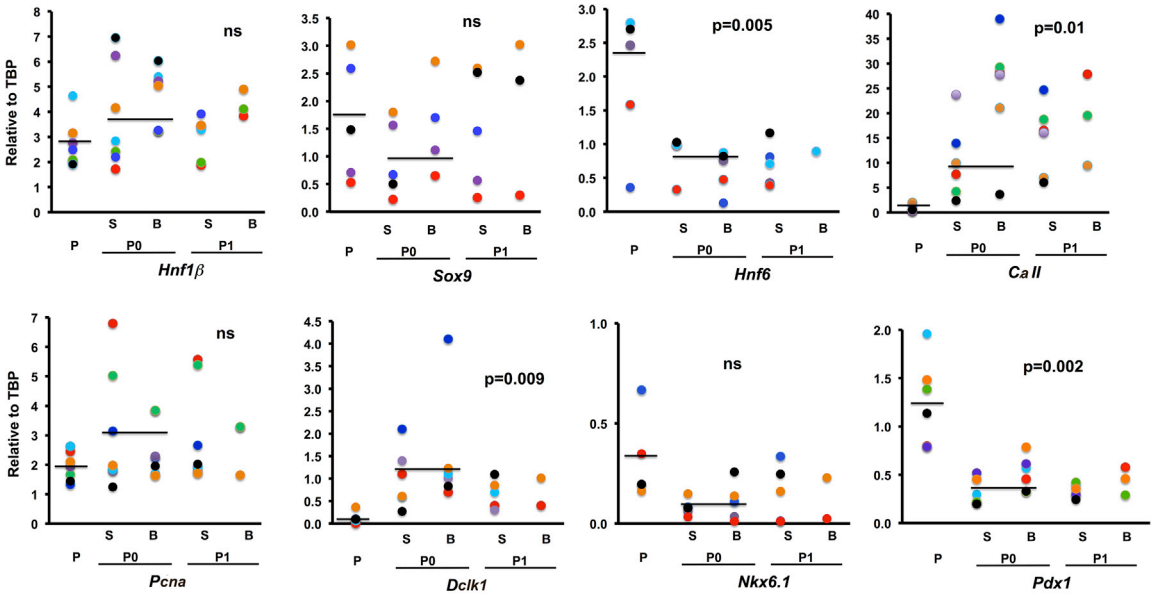

Figure 5. Organoids Maintain Expression of Ductal Markers after Passaging

Freshly isolated murine duct cells (P), handpicked organoids after 2 weeks (P0), and 7 days after first passage (P1) showed similar expression of *Sox9* and *Hnf1β* mRNA, whereas *Hnf6* and *Pdx1* decreased ($p < 0.005$), and *CaII* and *Dckl1* increased in organoids, compared with primary duct cells ($p < 0.01$). *Nkx6.1* expression did not differ; *Pcna* expression was highly variable. S, sphere; B, branched. Each experiment color coded. Means shown. p value compared P0 with P. ns, not significant. See also Figure S1.

(Figure 4D); those greater that 188 μm in diameter had approximately 45% Ki67$^+$ cells, whereas in smaller organoids (>38, <188 μm) only 8.5% had Ki67+, demonstrating a heterogeneity of their proliferation capacity (n = 3 isolations).

Hnf1β and *Sox9* Expression Was Maintained in Organoids Even after Passaging

We examined protein expression in whole-mount intact P2 organoids (21 days after isolation) by immunostaining for the key duct transcription factors SOX9, HNF1β, and HNF6 co-stained with Ki67. Clear heterogeneity within and among organoids was observed (Figures 4D and 4E). About 85% of the cells were positive for these transcription factors, whether high or low intensity. Interestingly, Ki67$^+$ cells (Figure 4E) had very low or undetectable expression of SOX9, HNF6, and HNF1β. Since these organoids developed from single cells, the protein expression must be transiently lost with replication, as suggested previously in the KGF experiment.

In addition, RNA was extracted from freshly purified CD24$^+$ duct cells, after a 2-week culture as organoids (P0), and 1 week after first passage (P1) (Figure 5). Organoids, both spheres and branched structures, at P0 and P1, had similar levels of *Sox9* and *Hnf1β* mRNA as freshly purified duct cells, but *Hnf6* and *Pdx1* were slightly decreased. Expressions of the differentiated duct marker *Carbonic anhydrase II* (*CaII*) and *Doublecortin-like kinase 1* (a putative pancreatic progenitor marker [Westphalen et al., 2016]) mRNAs were consistently induced in the organoids. *Pcna* and *Nkx6.1* expression varied across experiments. This maintenance of ductal characteristics in organoids contrasted to the considerable loss of duct genes in duct cells cultured as monolayers (Dodge et al., 2009) (Figure S1).

Cell Surface Molecules for Sorting HNF1β$^{high/low}$ and SOX9$^{high/low}$ Populations

CA19-9 and CD44/CD24 had been useful to purify duct cells from human and rodent, respectively, so we looked for additional cell surface proteins to sort live cells into subpopulations. Flow cytometry on CD44$^+$ mouse duct cells co-stained for HNF1β and CD24 showed that CD24 expression also overlapped with HNF1β expression (Table S2): 73.8% of CD24^{high} cells expressed HNF1β^{high}. Similar enrichment was seen for SOX9, 76.4% of CD24^{low} expressed SOX9^{low}. In humans, CD51 had a similarly selective but variable expression in ducts (Figures S2A and S2B). Flow cytometry on CA19-9-purified human ducts cells co-stained for HNF1β and CD51 showed that CD51 expression overlapped with HNF1β expression: 93.4% of CD51^{high} cells expressed HNF1β^{high}, and 71% of CD51^{low} expressed HNF1β^{low} (Figure S2C). Thus using one cell surface antibody to purify and another to sort subpopulations, pancreatic ducts could be sorted into the enriched

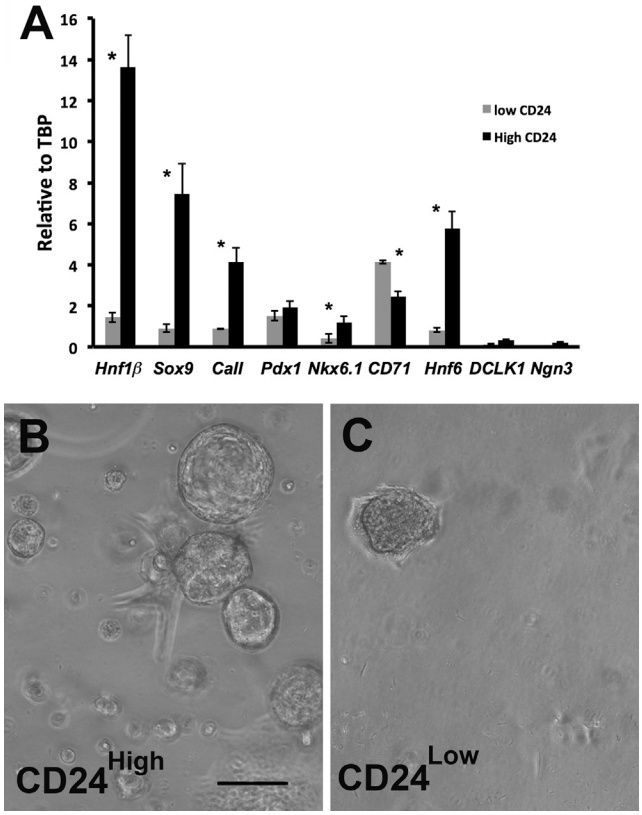

Figure 6. Two Distinct Populations within Duct Cells Based on CD24 Expression in CD44^{+} Purified Murine Duct Cells

(A) CD44^{+} purified duct cells FACS sorted with anti-CD24 antibody showed CD24^{high} and CD24^{low} populations with distinct gene expression patterns. n = 3 experiments, 5 mice each. See Tables S2 and S3. Similar data for human ducts (CD51) and for mouse (a second CD24 antibody) are shown in Figure S3. CD24^{high} duct cells were able to form organoids reproducibly (B), whereas CD24^{low} cells (C) formed few, if any, organoids after 1 week. n = 4 experiments. Data are means ± SEM. *p < 0.05. Scale bar, 200 μm.

subpopulations of expression levels of HNF1β and SOX9. We also sorted CD44^{+}-purified mouse ducts according to CD24 expression against cell granularity (side scatter) and observed multiple distinct populations (Figure S3). The populations sorted by CD24 against either size or granularity overlapped with each other, verifying that there were at least two distinct populations.

Using this FACS strategy, CD24^{high} and CD24^{low} living murine duct cells were collected for qPCR analysis (Figure 6A and S4). CD24^{high} cells had higher levels of *Hnf1β*, *Sox9, CaII*, *Hnf6, Hes1*, and *Notch2* mRNA than CD24^{low} cells, but had similar levels of *Pdx1* mRNA. *CD71* showed a higher expression in CD24^{low}. While the populations from young (7–8 weeks) and old mice (7–9 months) had similar gene expression patterns, CD24^{low} cells were twice as abundant in the younger animals (Table S3). These results show that the differential expression of CD24 is an appropriate surface marker to separate two distinct subpopulations, *Hnf1β* ^{low}*/Sox9* ^{low} and *Hnf1β*^{high}*/Sox9*^{high}. Similarly, CD51^{high} human duct cells had significantly higher *HNF1β* and *SOX9* mRNA than CD51^{low} cells, but *HES1*, *PDX1, HNF6*, and *NOTCH2* did not differ in the human sorted subpopulations (Figure S4).

Following these experiments, we wondered if these subpopulations differed in their organoid formation potential. Mouse duct cells were isolated by immunomagnetic separation with CD44 antibody, FACS sorted according to their CD24 expression (CD24$^{high/low}$), and then plated in Matrigel. After a 2-week culture only the CD24^{high} (*Hnf1β*^{high}*/Sox9*^{high}) subpopulation formed organoids robustly (Figure 6B), whereas few organoids were observed in CD24^{low} cells (Figure 6C). The formed organoids were able to make organoids when passaged.

Pancreatic Duct Cell-Derived Organoids Differentiated into Pancreatic Endocrine Progenitor Cells

During early pancreas development, PDX1 is expressed throughout the epithelium, diminishes in midgestation (Gu et al., 2002; Jensen et al., 2000), and then increases as cells differentiate toward β cells (MacFarlane et al., 1994). We hypothesized that the pancreatic duct-derived organoids, which had high expression of PDX1 protein, would be the equivalent of embryonic pancreatic progenitor cells. We used a 14-day stepwise differentiation protocol (Figure 7A) modified from the human embryonic stem cell (hESC) protocol of Rezania et al. (2014) on P2 duct organoids (n = 3 experiments). Organoids had a stable *Pdx1* mRNA expression through the differentiation protocol, with levels equal or greater than that of E16 mouse pancreas (Figure 7B). While NKX6.1 appears to be a marker of multipotent pancreatic progenitor cells, around E15 NKX6.1 expression becomes restricted to insulin-positive cells (Sander et al., 2000). In these treated organoids, *Nkx6.1* mRNA increased to about 25% of that of E16 pancreas (Figure 7B). Interestingly, *Ngn3* mRNA was induced significantly during the differentiation protocol ($p < 0.001$) (Figure 7B). In addition, *Mafb* mRNA, which is expressed in the earliest insulin-expressing cells, as well as the glucagon-expressing cells, was induced in stage 3 of our differentiation protocol ($p < 0.002$) (Figure 7B). Thus, the organoids expanded from *Hnf1β* ^{high}*Sox9*^{high} cells can be differentiated toward islet endocrine cells.

DISCUSSION

Using careful titration of antibodies for immunofluorescence and flow cytometry analysis, we have shown

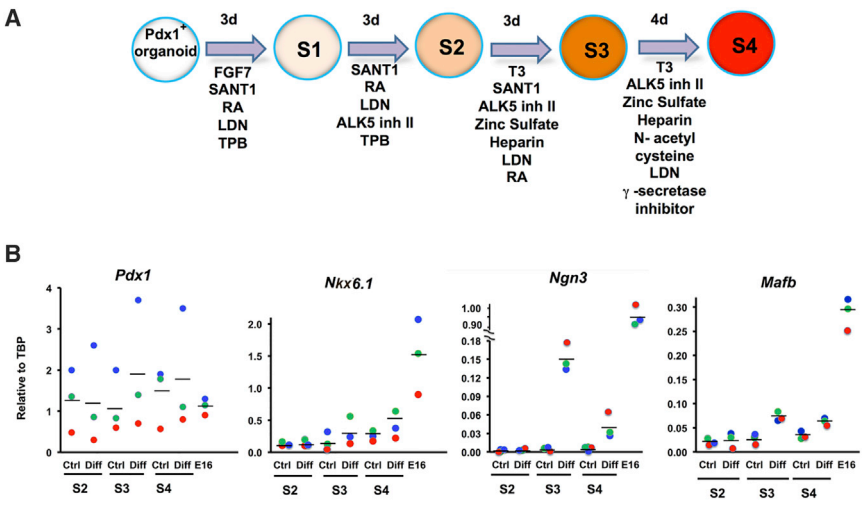

Figure 7. Organoids Can Differentiate to Endocrine Progenitor-like Cells

(A) Schematic of directed differentiation of P2 organoids to endocrine progenitor-like cells using protocol modified from Rezania et al. (2014).

(B) Through the protocol, organoids continued to express *Pdx1* mRNA at levels equal or greater than that of E16 pancreas, *Nkx6.1* mRNA expression increased, reaching 25% that of E16 pancreas, *Ngn3* mRNA ($p < 0.001$) and *Mafb* mRNA, which is expressed in the earliest insulin-expressing cells, were induced ($p < 0.002$). n = 3 experiments, color-coded. Ctrl, control; Diff, differentiation.

subpopulations of adult human and rodent pancreatic duct cells based on their expression of transcription factors HNF1β and SOX9. These subpopulations differ in location, proportions, and gene expression profiles. Studies with induced replication showed changes in the expression patterns, suggesting that these populations reflect distinct and dynamic differentiation states of the cells.

While both HNF1β and SOX9 had differential patterns of expression through the ductal tree in human and mouse pancreas, the patterns were unique for each transcription factor. The proportions of HNF1β and SOX9-expressing duct cells differed among human, mouse, and rat even though the isolated ducts were mainly from the smaller ducts in all three species. In a recent single-cell RNA sequencing study, Baron et al. (2016) reported at least two spatially distinct duct subpopulations with distinct transcriptomes in human and mouse.

Living *HNF1β^{high}* and *HNF1β^{low}* subpopulations could be sorted based on cell surface proteins in both human (CD51) and mouse (CD24). In these subpopulations, there were clear differences in expression of both *Hnf1β* and *Sox9*, but not of the other important duct transcription factor *Pdx1*. Genes that are associated with mature ducts, *CaII* and *Hnf6*, had higher expression in CD24^{high} cells. CD24, as well as *Sox9* and *Spp1* (Senkel et al., 2005), is a target of HNF1β; it is unclear if CD51 (integrin alpha V) was also an HNF1β target gene. CD24 is of particular interest as it is reported as a marker of pancreatic cancer stem cells (Li et al., 2007), tumorigenic human breast cancer cells (Al-Hajj et al., 2003), a biomarker for neural stem cells (Pruszak et al., 2009), and actively cycling intestinal epithelial stem cells (Gracz et al., 2010; von Furstenberg et al., 2011).

As previously shown, dissociated single cells from adult mouse pancreas (Bonner-Weir et al., 2010; Dorrell et al., 2014; Huch et al., 2013; Jin et al., 2016; Lee et al., 2013) and humans (Lee et al., 2013) can be expanded as *in vitro* organoids in Matrigel. We found about 15% of purified murine duct cells were able to form organoids that can become more than 400 μm in diameter and can be passaged. Yet, organoids were only formed from CD24^{high} cells. These cells also had lower expression of *CD71* mRNA, which would be consistent with the finding by the Ku group that CD133^{high} and CD71^{low} pancreatic cells were enriched in colony-forming units (Jin et al., 2016). More studies are needed to fully characterize these subpopulations.

Our results strongly support a dynamic expression of HNF1β and SOX9 in pancreatic duct cells that may reflect the state of differentiation of the duct cells. Duct cells in adult mice are quiescent for the most part, with only 2% of the ductal epithelial cells expressing Ki67. Yet, at 24 hr after stimulation with KGF, 18% of the duct cells were BrdU^{+} as the proportion of HNF1β^{high}- and SOX9^{high}-expressing cells fell; the BrdU^{+} cells had decreased expression of the transcription factors. Similarly, even though organoids only form from the CD24^{high} population that is enriched in *HNF1β^{high}* and *SOX9^{high}* cells, our whole-mount immunostaining of organoids showed a clear heterogeneity of the expression of HNF1β, SOX9, and HNF6 among organoids and within an organoid, with proliferating cells (Ki67^{+}) having low or undetectable expression of them. The loss of HNF1β and SOX9 with proliferation in ducts is consistent with our findings in the partial pancreatectomy regeneration model in adult rats. By 4 hr after surgery, there was a significant loss of *Hnf6* expression in ducts; within 16 hr, a loss of expression of *Hnf1β* and *Sox9* at both the mRNA and protein levels was seen and preceded extensive proliferation. In that model, the pancreatic duct cells

undergo dedifferentiation to a more progenitor-like state, proliferate, and then re-differentiate into pancreatic exocrine and endocrine cells forming whole new lobes of pancreas (Li et al., 2010).

The question is, then, do these findings help clarify the controversy of the lineage-tracing studies? The lineage-tracing experiments based on inducible *Hnf1β* and *Sox9 cre* (Kopp et al., 2011; Solar et al., 2009) did not find any islet or acinar cells labeled when tamoxifen was given at E18.5 and analysed in the first postnatal weeks. In the neonatal period there is massive growth of the pancreas so the lack of labeled acini is puzzling (Bonner-Weir et al., 2016). It would be reasonable to assume that HNF1β^{high} or SOX9^{high} expressers would be most likely to activate the *cre* transgene, even with low recombination efficiency. Our data on protein expression (Figure 2) showed only 30%–35% of the adult quiescent duct cells were high expressers of either SOX9 or HNF1β, and expression of HNF1β and SOX9 is dynamic and decreased with replication. Neonatal duct cells are highly replicative (about 20% Ki67 at 2 weeks and 8% Ki67 at 4 weeks) in contrast to the low ductal replication in adult mice (about 2% Ki67^{+}) (Guo et al., 2013). Perhaps the observed lack of labeled islet and acinar cells in neonatal *Hnf1β* and *Sox9 cre* mice was due to a paucity of high-expressing duct cells at time of activation. In contrast, CAII expression was expressed in the ducts starting at E18 and increased with age, so recombination would increase in the neonatal period in the constitutively active *CaIICre* mice in which both labeled islet and acinar cells were observed (Inada et al., 2008).

The resemblance of gene expression of organoids to embryonic pancreatic progenitors, including their high expression of PDX1 in P2 and P3, led us to test a short stepwise differentiation protocol on their potential to become pancreatic endocrine progenitors. After a 14-day differentiation protocol, P2 organoids had *Pdx1* mRNA equal or greater than that of E16 pancreas, *Nkx6.1* mRNA increased to about 25% of that E16 pancreas, and both *Neurogenin3* and *Mafb* mRNA were induced. These results, consistent with other studies (Bonner-Weir et al., 2004; Corritore et al., 2014; Jin et al., 2013; Yamada et al., 2015; Yatoh et al., 2007; Zhang et al., 2016), suggest the possibility of differentiating adult duct cells into pancreatic endocrine cells.

In conclusion, we show that both transcription factors HNF1β and SOX9 are differentially expressed through the pancreatic ductal tree and that their expression is dynamic with decreases after replication. In addition, we identified cell surface markers that can be used to sort the subpopulations of duct cells with different expression profiles and the potential to form organoid structures in a 3D environment. The current findings demonstrate subpopulations and heterogeneity within duct cells, and raise the question of whether only a subpopulation of adult pancreatic duct cells can serve as facultative progenitors.

EXPERIMENTAL PROCEDURES

Animals

Animals were kept under conventional conditions with free access to water and food. All animal procedures were approved by the Joslin Institutional Animal Care and Use Committee. For histology, pancreas was excised from anesthetized animals, fixed in 4% paraformaldehyde and embedded in paraffin. For the KGF experiment, 8-week-old male C57BL/B6J mice (Jackson Laboratory) had a single intraperitoneal injection of recombinant human KGF (3 mg/kg PeproTech; n = 9) or saline (n = 3). Eighteen hours later all mice received an injection of BrdU (Invitrogen, 90 mg/kg). At 24 hr (n = 3), 48 hr (n = 3), and 72 hr (n = 3) after KGF administration, and after 24 hr of saline, mice were anesthetized and pancreases excised.

Rodent Duct Isolation

Dispersed islet-depleted pancreatic tissue remaining after collagenase digestion for islet isolation (Gotoh et al., 1985) from adult mice and rats was collected from pools of 10–15 mice/rat per sample and divided into 50 mL conical tubes and suspended in RPMI 1640 medium (Invitrogen) supplemented with 10 μm EZSolution Y-27632 ROCK Inhibitor (BioVis) and RNasin Plus RNase Inhibitor (Promega, 100 μL:100 mL). After suspension, tissue was allowed to settle for 5 min, and the supernatant was aspirated to remove low-density components including dead cells and islets. For cell dispersion, 2 mL of 0.25% trypsin/EDTA solution (Invitrogen) and 20 mL PBS (Mg/Ca free) were added, vortexed for several seconds and incubated for 4 min at 37°C on 200 rpm in an incubator shaker. Cold RPMI 1640 medium was added to halt the enzymatic reaction. Following multiple washes and vortexing, tissue was filtered through 40 μm cell strainers (Falcon) to remove clumps. Dissociation into single cells was confirmed by light microscopy. Most acinar tissue (larger cells) was not viable at this stage, as assessed by trypan blue exclusion. Duct cells were then purified using MACS magnetic LS separation columns (Miltenyi Biotec) according to the manufacturer's instructions with anti-CD24 and/or anti-CD44 antibodies (Table S4 for antibodies).

Human Duct Isolation

After islet isolation by the Clinical Islet Transplantation Unit (Mass General Hospital), islet-depleted human pancreatic tissue was dispersed and incubated with CA19-9 and purified using MACS magnetic LS separation columns (Miltenyi Biotec) as described previously (Yatoh et al., 2007). De-identified organ donors (34–70 years) were non-diabetic and had research consent; exempt status was approved by the Joslin Institutional Review Board.

Flow Cytometry

For intracellular (nuclear) staining of duct cells, purified duct cells were washed in PBS and fixed at room temperature for

10 min in 4% formaldehyde fixation/permeabilization buffer (1 mL/10 million cells, Cytofix/Cytoperm BD), washed in PBS, and incubated overnight at 4°C with primary antibody diluted in perm/wash buffer. After wash in Perm/Wash buffer, they were incubated with secondary antibody conjugated to Alexa 647or Alexa 488 (1:800; Invitrogen) for 1.5 hr at room temperature in the dark on a rotary shaker. For co-staining with intracellular and surface molecule markers, cells were first incubated on ice for 15 min in cold PBS with fluorochrome-conjugated surface molecule antibody. Following the surface staining, cells were washed in cold PBS, resuspended with Fixation/Permeabilization buffer, and stained for the intracellular (nuclear) marker. Cells were resuspended in PBS and sorted using a FACSAria (Becton Dickinson, San Jose, CA). Expression gating was determined by using primary and unstained control to set the "undetectable" gating. Expressed cells were gated so that half were considered low expression. Results were analyzed using FlowJo flow cytometry analysis software.

For FACS sorting of live cells, cells were initially isolated as above. Some isolated cells were taken as a primary sample and the rest were blocked by rat anti-mouse CD16/CD32 (Mouse BD Fc Block, BD), then incubated with anti-CD24 or anti-CD51 resuspended in FACS buffer (5% fetal bovine serum [FBS] in PBS Mg/Ca free) for 1 hr. Cells were washed three times with FACS buffer and pass through 35 mm mesh and collected in a sterile round bottom tube (Fisher) on ice.

Organoid Culture and Passage

To assess the organoid formation efficiency of primary duct cells, 10,000 freshly isolated duct cells (using only anti-CD24 and immunobeads) were suspended in 100 μL of Matrigel Matrix GFR Phenol RF (Corning) and cultured in adDMEM/F12 medium (17.5 mM; Thermo Fisher Scientific) supplemented with R-spondin, Noggin, Wnt1, fibroblast growth factor 10, epidermal growth factor, and nicotinamide (modified from Lee et al., 2013; see Table S1). Fresh medium was replaced every 5 days. Images were taken systematically on Olympus CK2 inverted microscope. Organoids were counted manually and the percentage of formed organoid structures calculated.

For passaging organoids, medium was aspirated, wells washed with PBS (Mg/Ca free) and cold Corning Cell Recovery Solution added to each well. Then Matrigel was dispersed and transferred to a 15-mL tube. Organoids were broken apart by pipetting up and down 50 times with a tip-bent pipet. After 10 min on ice, the suspension was centrifuged and 2 mL trypsin (0.25%) added to each tube; after 3 min at 37°C, medium supplemented with FBS was added to neutralize the trypsin. Duct cells were then embedded in an appropriate volume of Matrigel and re-cultured at 1:3 ratio.

Immunohistochemistry and Image Processing

Primary antibodies (Table S4) were applied overnight in 4°C. All biotinylated and fluorescent-conjugated antibodies were from Jackson ImmunoResearch, streptavidin-conjugated Alexa Fluor 488 or 568 antibodies from Invitrogen. Antigen retrieval was performed using a pressure cooker or a microwave in citrate buffer, pH 6.0. Non-specific binding was blocked using an Avidin/Biotin Blocking Kit (Vector Laboratories). For whole-mount immunostaining, organoids were grown in 8-chamber polystyrene chamber slides (Falcon), fixed in 10% formalin for 30 min, and washed with PBS twice, each for 5 min. Cells were permeabilized with 0.1% saponin for 15 min followed by wash buffer (PBS + 2% lamb serum + 0.3% Triton X-100). Samples were then sequentially incubated (2 hr each) with biotin-conjugated donkey anti-rabbit immunoglobulin G (IgG), SA-Alexa Fluor 594, mouse anti-Ki67 antibody, and fluorescein isothiocyanate-conjugated anti-mouse IgG. Between steps, slides were washed three times, each for 15 min on a slow speed shaker. Nuclei were stained with mounting medium with DAPI (Vector Laboratories). Stained sections/organoids were examined on an Olympus BH-2 microscope or in confocal mode on a Zeiss LSM 410 or 710 microscope. Final images were compiled using Adobe Photoshop. Samples were stained and imaged with parallel parameters so the staining intensities reflex the protein levels. All immunostaining results were reproducibly examined with at least three independent samples unless otherwise stated. Assessment of immunostaining intensity was done "by eye." Ducts were categorized as large or small ducts based on the classic criteria of diameter, type of epithelium, and amount of stroma (Githens et al., 1980).

For quantification, stained duct cells were counted manually on confocal images taken from two sections of pancreas of each mouse; the common pancreatic ducts were excluded since they are not usually retrieved in the duct isolations. The number of $BrdU^+$ duct cells was scored as a percentage of the duct cells on a section (at least 1,400 duct cells counted per time point, n = 3 animals). The percentages of cells expressing high, low, and undetectable levels of HNF1β or SOX9 were quantified for $BrdU^+$ and $BrdU^-$ duct cells.

Differentiation of Duct Organoids to Pancreatic Endocrine Cells

For differentiation, P2 organoids, which highly express PDX1 protein, were considered equivalent to hESC stage 3 (Rezania et al., 2014), washed with PBS (Mg/Ca free), and changed to MCDB131 medium (Thermo Fisher Scientific) supplemented with compounds as listed in Table S5 for 3 days each for stage 1 (S1)–S3 and 6 days for S4. Medium was changed daily. Samples were taken from each step for RNA analysis. Control organoids were kept in MCDB131 medium supplemented with 1× GlutaMAX.

RNA and Real-Time qRT-PCR Analysis

Total RNA was extracted immediately after flow cytometry sorting with RNeasy Micro Kit (QIAGEN) and RNase-Free DNase (QIAGEN) according to the manufacturer's protocols. Purified RNA concentration was measured by a NanoDrop TM 1000 Spectrophotometer. Reverse transcription to cDNA was carried out using a High Capacity cDNA Reverse Transcription Kit (Applied Biosystems) or a QuantiTect Reverse Transcription Kit (QIAGEN) according to the manufacturer's protocol. Real-time qPCR was performed using ABI Prism SDS 7900 PCR and SYBR-based detection (Applied Biosystems). TATA box binding protein was used as internal control. Relative quantification delta Ct analysis was used to determine the relative expression of target genes between different samples. Primers are given in Table S6.

Statistical Analysis

All results are presented as mean ± SEM. Statview, ANOVA, and *post-hoc* paired comparisons (Fisher's PLSD test or Bonferroni) were done to compare percentage of cells in Figure 3 and mRNA levels in Figure 6.

SUPPLEMENTAL INFORMATION

Supplemental Information includes four figures and six tables and can be found with this article online at https://doi.org/10.1016/j.stemcr.2018.01.028.

AUTHOR CONTRIBUTIONS

H.R., L.O.-Y., and S.B.-W. conceived the project, researched data, and wrote the manuscript. C.A.K., B.A.S., J.H.-L., W.-C.L., and L.G. researched data. S.D., J.L., and J.M. provided high quality human tissue. All authors reviewed the manuscript.

ACKNOWLEDGMENTS

The authors thank Vaja Tchipashvili for expert technical help for obtaining mouse exocrine tissue and Joyce LaVecchio, Giri Buruzula, Angela Wood, and Sarah Harris for assistance with flow cytometry. Special thanks to David Breault for providing the NRW cell line generated by Dr. Stappenbeck (Miyoshi and Stappenbeck, 2013). This study was supported by grants from JDRF (34-2008-641) and from NIH Joslin Diabetes Research Center (P30 DK036836), the Diabetes Research & Wellness Foundation, and an important group of private donors. H.R. was supported in part by a fellowship from the Hahnemann Hospital Foundation.

Received: August 15, 2017
Revised: January 22, 2018
Accepted: January 24, 2018
Published: February 22, 2018

REFERENCES

Al-Hajj, M., Wicha, M.S., Benito-Hernandez, A., Morrison, S.J., and Clarke, M.F. (2003). Prospective identification of tumorigenic breast cancer cells. Proc. Natl. Acad. Sci. USA *100*, 3983–3988.

Al-Hasani, K., Pfeifer, A., Courtney, M., Ben-Othman, N., Gjernes, E., Vieira, A., Druelle, N., Avolio, F., Ravassard, P., Leuckx, G., et al. (2013). Adult duct-lining cells can reprogram into β-like cells able to counter repeated cycles of toxin-induced diabetes. Dev. Cell *26*, 86–100.

Baeyens, L., Lemper, M., Leuckx, G., De Groef, S., Bonfanti, P., Stange, G., Shemer, R., Nord, C., Scheel, D., Pan, F., et al. (2014). Transient cytokine treatment induces acinar cell reprogramming and regenerates functional β-cell mass in diabetic mice. Nat. Biotechnol. *32*, 76–83.

Baron, M., Veres, A., Wolock, S.L., Faust, A.L., Gaujoux, R., Vetere, A., Ryu, J.H., Wagner, B.K., Shen-Orr, S.S., Klein, A.M., et al. (2016). A single-cell transcriptomic map of the human and mouse pancreas reveals inter- and intra-cell population structure. Cell Syst. *3*, 346–360.e4.

Beer, R.L., Parsons, M.J., and Rovira, M. (2016). Centroacinar cells: at the center of pancreas regeneration. Dev. Biol. *413*, 8–15.

Bonner-Weir, S., Aguayo-Mazzucato, C., and Weir, G.C. (2016). Dynamic development of the pancreas from birth to adulthood. Ups. J. Med. Sci. *121*, 155–158.

Bonner-Weir, S., Li, W.-C., Ouziel-Yahalom, L., Guo, L., Weir, G.C., and Sharma, A. (2010). β-cell growth and regeneration:replication is only part of the story. Diabetes *59*, 2340–2348.

Bonner-Weir, S., Toschi, E., Inada, A., Reitz, P., Fonseca, S.Y., Aye, T., and Sharma, A. (2004). The pancreatic ductal epithelium serves as a potential pool of progenitor cells. Pediatr. Diabetes *5* (*Suppl 2*), 16–22.

Butler, A.E., Cao-Minh, L., Galasso, R., Rizza, R.A., Corradin, A., Cobelli, C., and Butler, P.C. (2010). Adaptive changes in pancreatic β-cell fractional area and β-cell turnover in human pregnancy. Diabetologia *53*, 2167–2176.

Cereghini, S., Ott, M.O., Power, S., and Maury, M. (1992). Expression patterns of vHNF1 and HNF1 homeoproteins in early postimplantation embryos suggest distinct and sequential developmental roles. Development *116*, 783–797.

Chera, S., Baronnier, D., Ghila, L., Cigliola, V., Jensen, J.N., Gu, G., Furuyama, K., Thorel, F., Gribble, F.M., Reimann, F., et al. (2014). Diabetes recovery by age-dependent conversion of pancreatic delta-cells into insulin producers. Nature *514*, 503–507.

Collombat, P., Xu, X., Ravassard, P., Sosa-Pineda, B., Dussaud, S., Billestrup, N., Madsen, O.D., Serup, P., Heimberg, H., and Mansouri, A. (2009). The ectopic expression of Pax4 in the mouse pancreas converts progenitor cells into α and subsequently β-cells. Cell *138*, 449–462.

Corritore, E., Dugnani, E., Pasquale, V., Misawa, R., Witkowski, P., Lei, J., Markmann, J., Piemonti, L., Sokal, E.M., Bonner-Weir, S., et al. (2014). β-cell differentiation of human pancreatic duct-derived cells after in vitro expansion. Cell. Reprogram. *16*, 456–466.

Courtney, M., Gjernes, E., Druelle, N., Ravaud, C., Vieira, A., Ben-Othman, N., Pfeifer, A., Avolio, F., Leuckx, G., Lacas-Gervais, S., et al. (2013). The inactivation of Arx in pancreatic α-cells triggers their neogenesis and conversion into functional β-like cells. PLoS Genet. *9*, e1003934.

Criscimanna, A., Speicher, J.A., Houshmand, G., Shiota, C., Prasadan, K., Ji, B., Logsdon, C.D., Gittes, G.K., and Esni, F. (2011). Duct cells contribute to regeneration of endocrine and acinar cells following pancreatic damage in adult mice. Gastroenterology *141*, 1451–1462.

Dodge, R., Loomans, C., Sharma, A., and Bonner-Weir, S. (2009). Developmental pathways during in vitro progression of human islet neogenesis. Differentiation *77*, 135–147.

Dor, Y., Brown, J., Martinez, O.I., and Melton, D.A. (2004). Adult pancreatic beta-cells are formed by self-duplication rather than stem-cell differentiation. Nature *429*, 41–46.

Dorrell, C., Tarlow, B., Wang, Y., Canaday, P.S., Haft, A., Schug, J., Streeter, P.R., Finegold, M.J., Shenje, L.T., Kaestner, K.H., et al. (2014). The organoid-initiating cells in mouse pancreas and liver are phenotypically and functionally similar. Stem Cell Res. *13*, 275–283.

Furuyama, K., Kawaguchi, Y., Akiyama, H., Horiguchi, M., Kodama, S., Kuhara, T., Hosokawa, S., Elbahrawy, A., Soeda, T., Koizumi, M., et al. (2011). Continuous cell supply from a Sox9-expressing progenitor zone in adult liver, exocrine pancreas and intestine. Nat. Genet. *43*, 34–41.

Githens, S., 3rd, Holmquist, D.R., Whelan, J.F., and Ruby, J.R. (1980). Characterization of ducts isolated from the pancreas of the rat. J. Cell Biol. *85*, 122–135.

Gotoh, M., Maki, T., Kiyoizumi, T., Satomi, S., and Monaco, A.P. (1985). An improved method for isolation of mouse pancreatic islets. Transplantation *40*, 437–438.

Gracz, A.D., Ramalingam, S., and Magness, S.T. (2010). Sox9 expression marks a subset of CD24-expressing small intestine epithelial stem cells that form organoids in vitro. Am. J. Physiol. Gastrointest. Liver Physiol. *298*, G590–G600.

Gu, G., Dubauskaite, J., and Melton, D.A. (2002). Direct evidence for the pancreatic lineage: NGN3+ cells are islet progenitors and are distinct from duct progenitors. Development *129*, 2447–2457.

Guo, L., Inada, A., Aguayo-Mazzucato, C., Hollister-Lock, J., Fujitani, Y., Weir, G.C., Wright, C.V., Sharma, A., and Bonner-Weir, S. (2013). PDX1 in ducts is not required for postnatal formation of β-cells but is necessary for their subsequent maturation. Diabetes *62*, 3459–3468.

Huch, M., Bonfanti, P., Boj, S.F., Sato, T., Loomans, C.J., van de Wetering, M., Sojoodi, M., Li, V.S., Schuijers, J., Gracanin, A., et al. (2013). Unlimited in vitro expansion of adult bi-potent pancreas progenitors through the Lgr5/R-spondin axis. EMBO J. *32*, 2708–2721.

Inada, A., Nienaber, C., Katsuta, H., Fujitani, Y., Levine, J., Morita, R., Sharma, A., and Bonner-Weir, S. (2008). Carbonic anhydrase II-positive pancreatic cells are progenitors for both endocrine and exocrine pancreas after birth. Proc. Natl. Acad. Sci. USA *105*, 19915–19919.

Jensen, J., Heller, R.S., Funder-Nielsen, T., Pedersen, E.E., Lindsell, C., Weinmaster, G., Madsen, O.D., and Serup, P. (2000). Independent development of pancreatic α and β-cells from Neurogenin3-expressing precursors: a role for the notch pathway in repression of premature differentiation. Diabetes *49*, 163–176.

Jin, L., Feng, T., Shih, H.P., Zerda, R., Luo, A., Hsu, J., Mahdavi, A., Sander, M., Tirrell, D.A., Riggs, A.D., et al. (2013). Colony-forming cells in the adult mouse pancreas are expandable in Matrigel and form endocrine/acinar colonies in laminin hydrogel. Proc. Natl. Acad. Sci. USA *110*, 3907–3912.

Jin, L., Gao, D., Feng, T., Tremblay, J.R., Ghazalli, N., Luo, A., Rawson, J., Quijano, J.C., Chai, J., Wedeken, L., et al. (2016). Cells with surface expression of $CD133^{high}CD71^{low}$ are enriched for tripotent colony-forming progenitor cells in the adult murine pancreas. Stem Cell Res. *16*, 40–53.

Kopp, J.L., Dubois, C.L., Schaffer, A.E., Hao, E., Shih, H.P., Seymour, P.A., Ma, J., and Sander, M. (2011). Sox9+ ductal cells are multipotent progenitors throughout development but do not produce new endocrine cells in the normal or injured adult pancreas. Development *138*, 653–665.

Kushner, J.A., Weir, G.C., and Bonner-Weir, S. (2010). Ductal origin hypothesis of pancreatic regeneration under attack. Cell Metab. *11*, 2–3.

Lee, J., Sugiyama, T., Liu, Y., Wang, J., Gu, X., Lei, J., Markmann, J.F., Miyazaki, S., Miyazaki, J.I., Szot, G.L., et al. (2013). Expansion and conversion of human pancreatic ductal cells into insulin-secreting endocrine cells. Elife *2*, e00940.

Li, C., Heidt, D.G., Dalerba, P., Burant, C.F., Zhang, L., Adsay, V., Wicha, M., Clarke, M.F., and Simeone, D.M. (2007). Identification of pancreatic cancer stem cells. Cancer Res. *67*, 1030–1037.

Li, W.C., Rukstalis, J.M., Nishimura, W., Tchipashvili, V., Habener, J.F., Sharma, A., and Bonner-Weir, S. (2010). Activation of pancreatic-duct-derived progenitor cells during pancreas regeneration in adult rats. J. Cell Sci. *123* (Pt 16), 2792–2802.

Lynn, F.C., Smith, S.B., Wilson, M.E., Yang, K.Y., Nekrep, N., and German, M.S. (2007). Sox9 coordinates a transcriptional network in pancreatic progenitor cells. Proc. Natl. Acad. Sci. USA *104*, 10500–10505.

MacFarlane, W.M., Read, M.L., Gilligan, M., Bujalska, I., and Docherty, K. (1994). Glucose modulates the binding activity of the β-cell transcription factor IUF1 in a phosphorylation-dependent manner. Biochem. J. *303* (Pt 2), 625–631.

Mezza, T., Muscogiuri, G., Sorice, G.P., Clemente, G., Hu, J., Pontecorvi, A., Holst, J.J., Giaccari, A., and Kulkarni, R.N. (2014). Insulin resistance alters islet morphology in nondiabetic humans. Diabetes *63*, 994–1007.

Miyoshi, H., and Stappenbeck, T.S. (2013). In vitro expansion and genetic modification of gastrointestinal stem cells in spheroid culture. Nat. Protoc. *8*, 2471–2482.

Pan, F., Bankaitis, E., Boyer, D., Xu, X., Van deCasteele, M., Magnuson, M., Heimberg, H., and Wright, C. (2013). Spatiotemporal patterns of multipotentiality in Ptf1a-expressing cells during pancreas organogenesis and injury-induced facultative restoration. Development *140*, 751–764.

Pruszak, J., Ludwig, W., Blak, A., Alavian, K., and Isacson, O. (2009). CD15, CD24, and CD29 define a surface biomarker code for neural lineage differentiation of stem cells. Stem Cells *27*, 2928–2940.

Rezania, A., Bruin, J.E., Arora, P., Rubin, A., Batushansky, I., Asadi, A., O'Dwyer, S., Quiskamp, N., Mojibian, M., Albrecht, T., et al. (2014). Reversal of diabetes with insulin-producing cells derived in vitro from human pluripotent stem cells. Nat. Biotechnol. *32*, 1121–1133.

Rovira, M., Scott, S.G., Liss, A.S., Jensen, J., Thayer, S.P., and Leach, S.D. (2010). Isolation and characterization of centroacinar/terminal ductal progenitor cells in adult mouse pancreas. Proc. Natl. Acad. Sci. USA *107*, 75–80.

Sander, M., Sussel, L., Conners, J., Scheel, D., Kalamaras, J., Dela Cruz, F., Schwitzgebel, V., Hayes-Jordan, A., and German, M. (2000). Homeobox gene Nkx6.1 lies downstream of Nkx2.2 in the major pathway of β-cell formation in the pancreas. Development *127*, 5533–5540.

Seaberg, R.M., Smukler, S.R., Kieffer, T.J., Enikolopov, G., Asghar, Z., Wheeler, M.B., Korbutt, G., and van der Kooy, D. (2004). Clonal identification of multipotent precursors from adult mouse

pancreas that generate neural and pancreatic lineages. Nat. Biotechnol. *22*, 1115–1124.

Senkel, S., Lucas, B., Klein-Hitpass, L., and Ryffel, G.U. (2005). Identification of target genes of the transcription factor HNF1β and HNF1α in a human embryonic kidney cell line. Biochim. Biophys. Acta *1731*, 179–190.

Seymour, P.A., Freude, K.K., Dubois, C.L., Shih, H.P., Patel, N.A., and Sander, M. (2008). A dosage-dependent requirement for Sox9 in pancreatic endocrine cell formation. Dev. Biol. *323*, 19–30.

Seymour, P.A., Freude, K.K., Tran, M.N., Mayes, E.E., Jensen, J., Kist, R., Scherer, G., and Sander, M. (2007). SOX9 is required for maintenance of the pancreatic progenitor cell pool. Proc. Natl. Acad. Sci. USA *104*, 1865–1870.

Solar, M., Cardalda, C., Houbracken, I., Martin, M., Maestro, M.A., De Medts, N., Xu, X., Grau, V., Heimberg, H., Bouwens, L., et al. (2009). Pancreatic exocrine duct cells give rise to insulin-producing β-cells during embryogenesis but not after birth. Dev. Cell *17*, 849–860.

Teta, M., Long, S.Y., Wartschow, L.M., Rankin, M.M., and Kushner, J.A. (2005). Very slow turnover of β-cells in aged adult mice. Diabetes *54*, 2557–2567.

Teta, M., Rankin, M.M., Long, S.Y., Stein, G.M., and Kushner, J.A. (2007). Growth and regeneration of adult β-cells does not involve specialized progenitors. Dev. Cell *12*, 817–826.

Thorel, F., Nepote, V., Avril, I., Kohno, K., Desgraz, R., Chera, S., and Herrera, P.L. (2010). Conversion of adult pancreatic α-cells to β-cells after extreme β-cell loss. Nature *464*, 1149–1154.

von Furstenberg, R.J., Gulati, A.S., Baxi, A., Doherty, J.M., Stappenbeck, T.S., Gracz, A.D., Magness, S.T., and Henning, S.J. (2011). Sorting mouse jejunal epithelial cells with CD24 yields a population with characteristics of intestinal stem cells. Am. J. Physiol. Gastrointest. Liver Physiol. *300*, G409–G417.

Wang, C.Y., Gou, S.M., Liu, T., Wu, H.S., Xiong, J.X., Zhou, F., and Tao, J. (2008). Differentiation of CD24- pancreatic ductal cell-derived cells into insulin-secreting cells. Dev. Growth Differ. *50*, 633–643.

Westphalen, C.B., Takemoto, Y., Tanaka, T., Macchini, M., Jiang, Z., Renz, B.W., Chen, X., Ormanns, S., Nagar, K., Tailor, Y., et al. (2016). Dclk1 defines quiescent pancreatic progenitors that promote injury-induced regeneration and tumorigenesis. Cell Stem Cell *18*, 441–455.

Xu, X., D'Hoker, J., Stange, G., Bonne, S., De Leu, N., Xiao, X., Van De Casteele, M., Mellitzer, G., Ling, Z., Pipeleers, D., et al. (2008). β-cells can be generated from endogenous progenitors in injured adult mouse pancreas. Cell *132*, 197–207.

Yamada, T., Cavelti-Weder, C., Caballero, F., Lysy, P.A., Guo, L., Sharma, A., Li, W., Zhou, Q., Bonner-Weir, S., and Weir, G.C. (2015). Reprogramming mouse cells with a pancreatic duct phenotype to insulin-producing β-like cells. Endocrinology *156*, 2029–2038.

Yatoh, S., Dodge, R., Akashi, T., Omer, A., Sharma, A., Weir, G.C., and Bonner-Weir, S. (2007). Differentiation of affinity-purified human pancreatic duct cells to β-cells. Diabetes *56*, 1802–1809.

Yoneda, S., Uno, S., Iwahashi, H., Fujita, Y., Yoshikawa, A., Kozawa, J., Okita, K., Takiuchi, D., Eguchi, H., Nagano, H., et al. (2013). Predominance of β-cell neogenesis rather than replication in humans with an impaired glucose tolerance and newly diagnosed diabetes. J. Clin. Endocrinol. Metab. *98*, 2053–2061.

Zhang, M., Lin, Q., Qi, T., Wang, T., Chen, C.C., Riggs, A.D., and Zeng, D. (2016). Growth factors and medium hyperglycemia induce Sox9+ ductal cell differentiation into β-cells in mice with reversal of diabetes. Proc. Natl. Acad. Sci. USA *113*, 650–655.

Stem Cell Reports, Volume *10*

Supplemental Information

Heterogeneity of SOX9 and HNF1β in Pancreatic Ducts Is Dynamic

Habib Rezanejad, Limor Ouziel-Yahalom, Charlotte A. Keyzer, Brooke A. Sullivan, Jennifer Hollister-Lock, Wan-Chun Li, Lili Guo, Shaopeng Deng, Ji Lei, James Markmann, and Susan Bonner-Weir

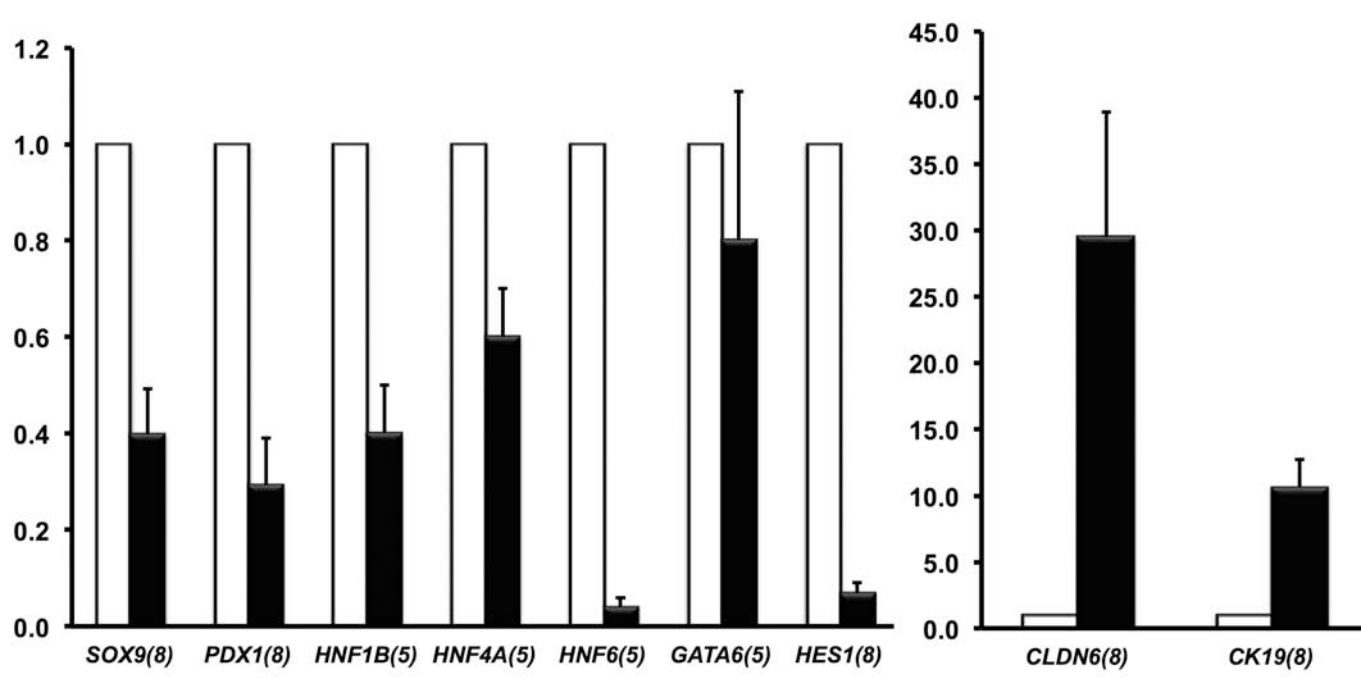

Figure S1 related to Figure 5. Purified human ducts lose ductal characteristics when cultured 1 week as monolayers. CA19.9 purified human ducts cultured as monolayer in CRML media for 1 wk (black bars) lose their ductal phenotype compared to the freshly isolated cells (white bars). The values are normalized to that of fresh ducts of the same donor; the number of donors in parentheses. The Ct values were: 20 for *HES*, 24 for *PDX*1, 20 for *SOX9* but embryonically expressed *claudin6* 25 for fresh but 19 for cultured. Mean±sem.

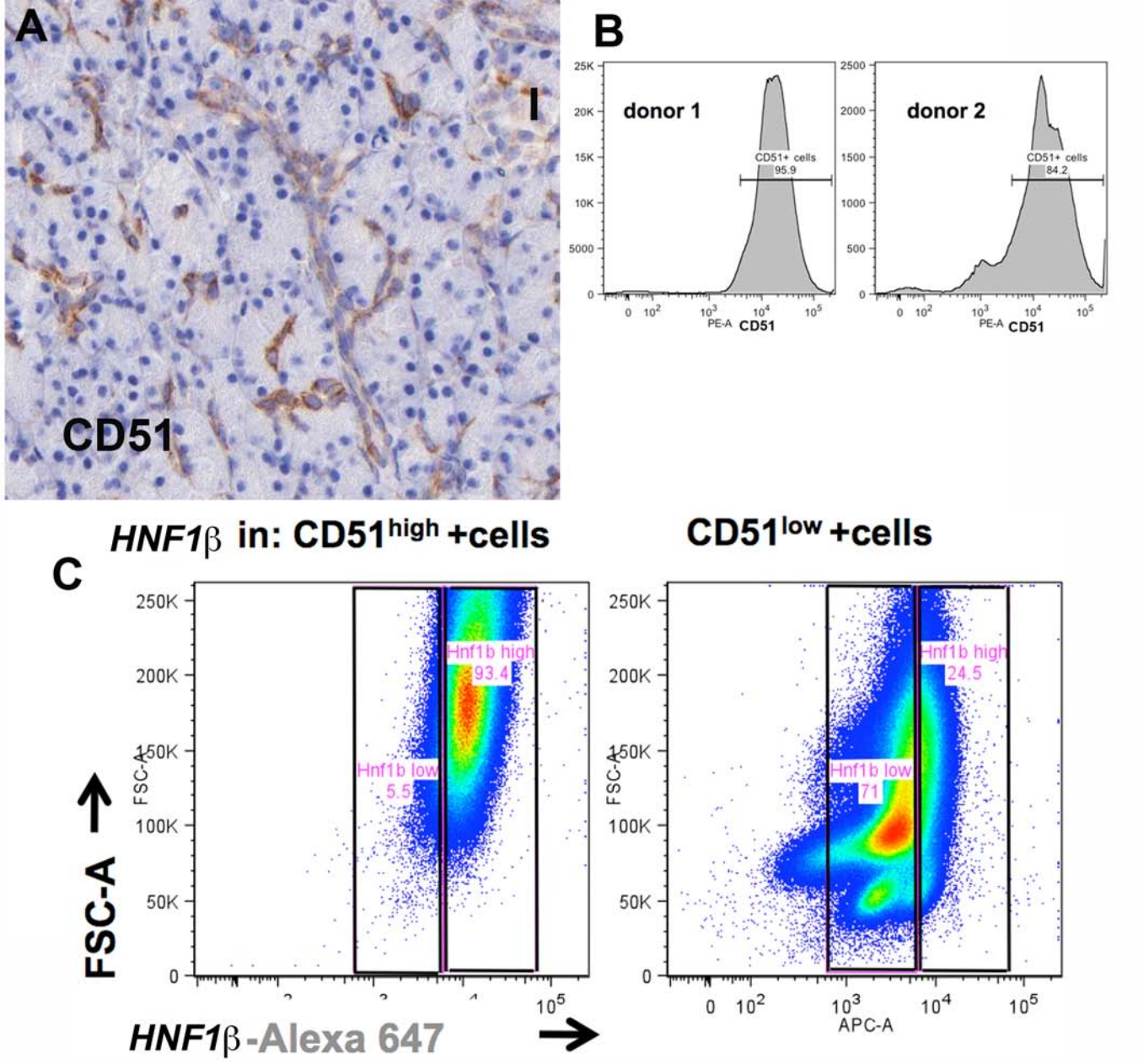

Figure S2 related to Figure 6. CD51 as second antibody for sorting human pancreatic duct cells. Based on our unpublished microarray data on human ducts (data not shown) and the immunostaining from the Human Protein Atlas (image from www.proteinatlas.org)**(A)**, CD51 had a specific but variable expression in ducts. We tested CD51 for sorting CA19-9 purified human pancreatic duct cells (**B**). As shown for two donors, the overlap was high with 95.9 and 84.2% overlap. **C.** Combined with immunostaining for HNF1β, CD51 expression largely overlapped with HNF1β expression: 93.4% of CD51^{high} cells expressed HNF1β^{high}, and 71% of CD51^{low} expressed HNF1β^{low}

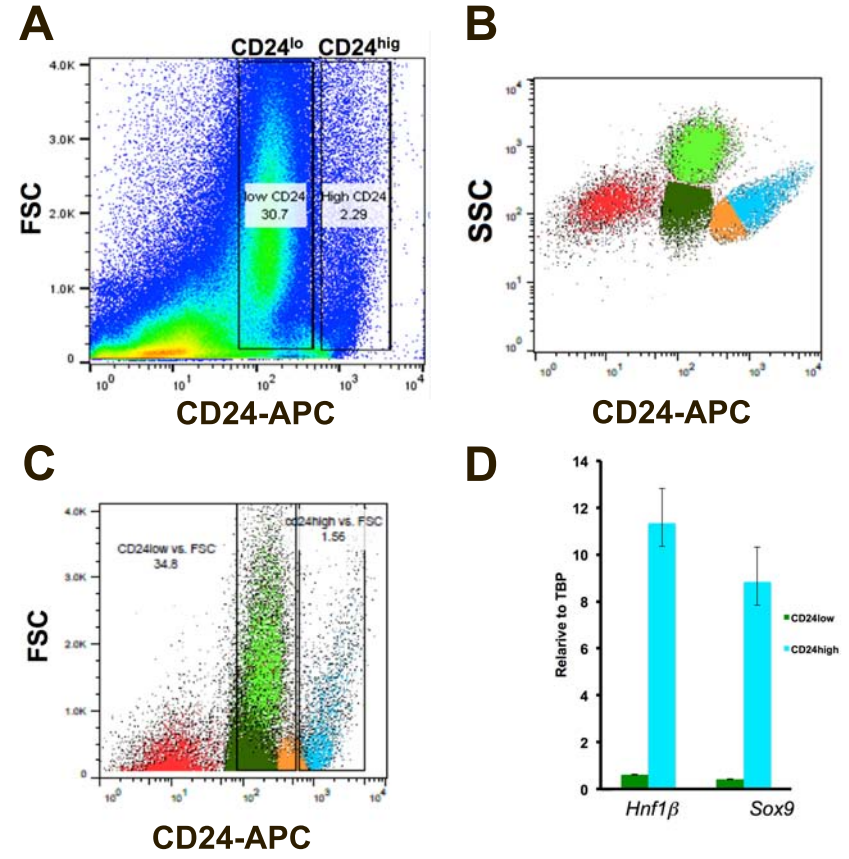

Figure S3 related to Figure 6. Alternate sorting strategy also indicates at least two populations. Mouse pancreatic ducts purified on basis of CD44+ using MACs were analyzed by FACS for the second antibody CD24. As shown in **A,** when plotted as increasing CD24 expression vs forward scatter FSC (size) as our usual protocol, we could "arbitrarily" assign high or low CD24 populations. **B** shows the same preparation but plotted as CD24 vs side scatter SSC (granularity) has clearly separate populations: red - $CD24^{negative}granularity^{low}$, dark green-$CD24^{low}granularity^{low}$, light green $CD24^{low}granularity^{high}$ and orange/aqua-$Cd24^{high}granularity^{low}$. **C** shows the overlap when these populations are plotted by FSC. When the cells were sorted on basis of CD24 vs SSC as either the green or aqua+orange populations, there was enrichment of *Hnf1β* and *Sox9* mRNA in the $CD24^{high}$ population (**D**). n= 3 experiments Mean±sem

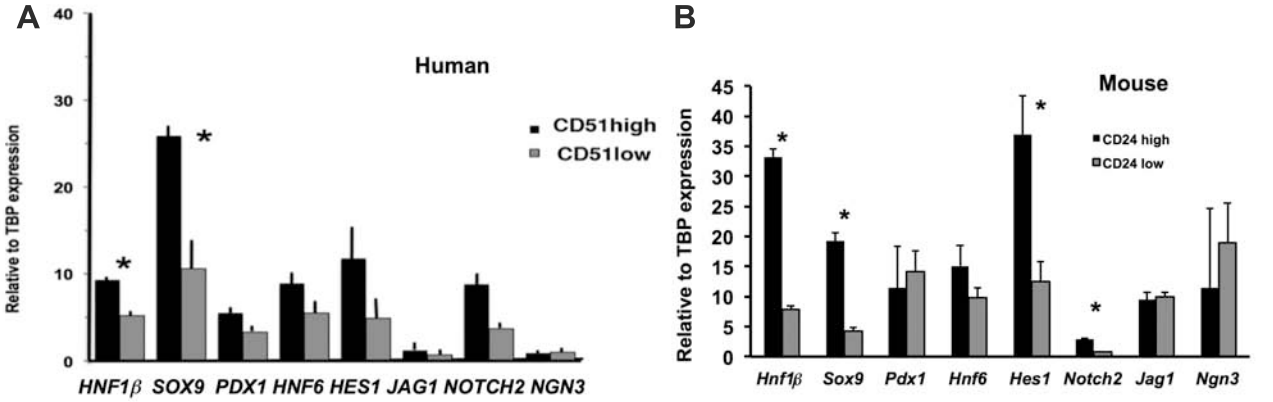

Figure S4 related to Figure 6. Gene expression in live pancreatic duct cells FACS sorted on the basis of 2 antibodies, first one to purify duct cells from islet-depleted tissue and second one to sort distinct subpopulations. **A.** Human duct cells were purified as CA19-9+ and subsequently incubated with CD51-PE and FACS sorted for $CD51^{high}$ and $CD51^{low}$ populations and finally their gene expression was analyzed by qPCR. Human pancreas donors(n=3), normalized to *TBP*. **B.** A second independent set of gene expression experiments on mouse duct cells purified by CD44 and the sorted for $CD24^{high}$ and $CD24^{low}$ using a different CD24-Pe antibody than in Figure 6. n=3 independent experiments, each pooled from 15 mouse pancreas; values normalized to *Tbp*. Mean ±sem

Table S1. Related to Experimental Procedures. Optimized organogenesis media for growing mouse pancreatic duct cell-derived organoids

Reagent	Concentration
Advanced DMEM/F12	50%
L-NRW cell line condition media	50%
Penicillin/Streptomycin	1X
FBS	10%
Glutamax	1X
FGF10	50 ng/ml
EGF	50 ng/ml
Nicotinamide	10 mM

Table S2. Related to Figure 6. Gating on CD24 expression of mouse CD44^{+} purified duct cells gave distinct subpopulations.

	CD24^{high}	**CD24^{low}**
% HNF1β ^{high}	73.8	55.8
%HNF1β ^{low}	24.7	34.7
%HNF1β ^{undetectable}	0.06	6.7
%SOX9 ^{high}	65.7	9.9
%SOX9 ^{low}	26.8	76.4
% SOX9 ^{undetectable}	0.05	9.6

Table S3. Related to Figure 6. $CD24^{low/high}$ subpopulations percentage between young and old mice. $CD24^{low}$ cells were twice as abundant in the younger animals.

Age	CD24 level	Percentage
Young (7-9 wks)	$CD24^{low}$	18.6
	$CD24^{high}$	1.2
Old (7-9 month)	$CD24^{low}$	8.7
	$CD24^{high}$	1.2
Old (1+year)	$CD24^{low}$	7.9
	$CD24^{high}$	2.5

Table S4. Related to Experimental Procedures. Primary antibodies used for different experiments

Application	Name	Derived species	Vendor	Catalogue #	Dilution (Method)
Duct cell isolation	CD24, clone M1/69	Rat	eBioscience	17-0242	1:100 (IMS)
	CD44	Rat	eBioscience	11-0441	1:100 (IMS)
	CA19-9	Mouse	Invitrogen	MA5-12421	1:100 (IMS)
FACS	HNF1β	Rabbit	Santa Cruz	SC8986	1:150 (PF)
	SOX9	Rabbit	Millipore	AB5535	1:1000 (PF)
	Fluorochrome-Conjugated-CD44clone IM7 PE	Rat	eBioscience	11-0441	1:100
	Fluorochrome-Conjugated-CA19-9	Mouse	Life Technologies	18-7240	1:200
	Fluorochrome-Conjugated-CD24, clone M1/69 APC	Rat	eBioscience	17-0242	1:100
	Fluorochrome-Conjugated- CD51	Mouse	eBioscience	12-0512	1:100
	CD16/CD32	Rat	BD	553142	1:100
IHC	HNF1β	Rabbit	Santa Cruz	SC22840; SC8986	1:150 (PF)
	HNF1β	Goat	Santa Cruz	SC7411	1:100 (PF)
	SOX9	Rabbit	Millipore	AB5535	1:1000 (PF)
	BrdU	Mouse	Dako	M0744	1:100 (PF)
	PanCK	Rabbit	Dako	Z0622	1:300 (PF)
Organoid staining	SOX9	Rabbit	Millipore	AB5535	1:200 (WM,Bio-SA)
	HNF1β	Rabbit	Santa Cruz	SC8986	1:200 (WM,Bio-SA)
	HNF6	Rabbit	Santa Cruz	13050	1:200 (WM,Bio-SA)
	Ki67	Mouse	BD Pharmigen	556003	1:200 (WM,FITC)

Abbreviations: IMS, Immunomagnetic Separation. Bio-SA, biotin-streptavidin-conjugated fluorescein amplification. PF, Paraffin Fixed. WM, Whole mount staining.

Table S5. Related to Experimental Procedures. MCDB131 media was supplemented with compounds listed for each stage (S1-S4) for differentiation of pancreatic duct cells-derived organoids to pancreatic progenitor cells.

Compound	Provider	Cat#	S1(d1-3)	S2(d3-6)	S3(d6-9)	S4 (d9-14)
Sodium bicarbonate	Sigma	S6297	2.5 g/l	2.5 g/l	1.5 g/l	1.5 g/l
Glutamax	Life Technologies	35050-061	1x	1x	1x	1x
Glucose	Sigma	G8769	10 mM	10 mM	20 mM	20 mM
BSA	Sigma	A2934	2%	2%	2%	2%
Ascorbic acid	Sigma	A4544	0.25 mM	0.25 mM	-	-
FGF7	R & D Systems	251-KG	50 ng/ml	2 ng/ml	-	-
SANT-1	Sigma	S4572	0.25 mM	0.25 mM	0.25 mM	-
Retinoic acid	Sigma	R2625	1 mM	0.1 mM	0.05 mM	-
Stemolecule™ LDN-193189	Stemgent	04-0019	100 nM	200 nM	100 nM	100 nM
Insulin-Transferrin-Selenium (ITS)	Life Technologies	51500056	1:200	1:200	1:200	1:200
PKC activator (TPB)	EMD Millipore	565740	200 nM	100 nM	-	-
3,3′5-Triiodo-l-thyronine sodium (T3)	Sigma	T6397	-	-	1mM	1mM
ALK5 inhibitor II	Enzo Life Sciences	AL X-270-445-M005	-	-	10 mM	10 mM
Zinc sulfate	Sigma	Z0251	-	-	10 mM	10 mM
Heparin	Sigma	H3149	-	-	10 mg/ml	10 mg/ml (d12-14)
γ-secretase inhibitor XX	EMD Millipore	565789	-	-	-	100 nM (d9-12)

Table S6. List of Primers, related to Experimental Procedures

Primer	**Sequence 5' to 3'** **forward**	**reverse**
Human		
SOX9	AAAGGCAACTCGTACCCAAATTT	AGTGGGTAATGCGCTTGGAT
PDX1	CTGGATTGGCGTTGTTTGTG	CCAAGGTGGAGTGCTGTAGGA
HNF1β	AGAAGCGTGCCGCTCTGT	GAATTGTCGGAGGATCTCTCGTT
HNF4a	CTGCAGGCTCAAGAAATGCTT	TCATTCTGGACGGCTTCCTT
GATA6	AGCGCGTGCCTTCATCA	GTGGTAGTTGTGGTGTGACAGTTG
HES1	TCCGGAGCTGGTGCTGAT	CCAGGACCAAGGAGAGAGGTAGA
CK19	GAAGGATGCTGAAGCCTGGTT	GCGACCTCCCGGTTCAAT
HNF6	GCAGGAAAACACCACTGGATCT	GCCAAGCACAGCGAGGAT
JAG1	AAAGATCTCAATTACTGTGGGACTCA	AGGGCCTGTGTTGCTACAAGTT
NGN3	TTTTGCGCCGGTAGAAAGG	CTCACGGGTCACTTGGACAGT
NOTCH 2	CCTTTTAGATGATAATGGACAACTATAGACTT	TGCCAAGAGCATGAATACAGAGA
CLDN6	GGA TCT TGA CAT GCC CAT CTT AG	CAA GCA GCC TCC GCA TTA G
RPLP0	CATCTACAACCCTGAAGTGCTTGA	ACCCTCCAGGAAGCGAGAAT
PPIA	GCGTCTCCTTTGAGCTGTTTG	CAGTGCTCAGAGCACGAAAATT
TBP	GCTTCCGCTGGCCCATA	ACGCCAAGAAACAGTGATGCT
Mouse		
Sox9	CGGCTCCAGCAAGAACAAG	GCGCCCACACCATGAAG
Pdx1	GATGTTGAACTTGACCGAGAGA	GTCCCGCTACTACGTTTCTTATC
Hnf1β	CCTCTCTCAACACCTCAACAAG	GAGGATCTCCCGTTGCTTTC
Hnf4a	CAAGAGGTCCATGGTGTTTAAGG	GTGCCGAGGGACGATGTAGT
Hes1	ACCCCAGCCAGTGTCAACA	TGTGCTCAGAGGCCGTCTT
Nkx6.1	CTTCTGGCCCGGAGTGATG	GGGTCTGGTGTGTTTTCTCTTC
CaII	CGATCCTTGCTCCCTTCTTC	CACGATCCAGGTCACACATT
Hnf6	AAGTTCCCTCACCAT CATCAC	AGTGTGAAACTACCGCTCAC
Pcna	CTCCGCCACCATGTTTGAG	CAGCACCTTCTTCAGGATGGA
Dclk1	CAGCCTGGACGAGCTGGTGG	TGACCAGTTGGGGTTCACAT
CD71	GAAGTCCAGTGTGGGAACAGGT	CAACCACTCAGTGGCACCAACA
Mafb	GCCTTCTTCTCCCAGCTTCA	ATCCAGTACAGGTCCTCGAGATG
Jag1	ACACAGGGATTGCCCACTTC	AGCCAAAGCCATAGTAGTGGTCAT
Ngn3	CAGTCACCCACTTCTGCTTC	GAGTCGGGAGAACTAGGATG
Notch 2	AGAGATGGAAGTGCCTATCACACA	GGACGGGACGTCTCTTCATTT
Tbp	CTGGCGGTTTGGCTAGGTT	TGGGCACTGCGGAGAAA